EVALUATION OF MODE-I FRACTURE OF CONCRETE-FRP BONDED INTERFACES USING THREE-POINT BENDING TESTS

Pizhong Qiao, Yingwu Xu, The University of Akron, Akron, OH
Julio F. Davalos, West Virginia University, Morgantown, WV

Abstract

Fiber-Reinforced plastic (FRP) composites are increasingly used in rehabilitation and strengthening of concrete structures, and significant increases in stiffness, strength and seismic response have been achieved. In this study, a conventional test method based on a three-point bending beam (3PBB) specimen, used commonly for determining Mode-I fracture properties of concrete and rock, is adapted to characterize Mode-I fracture of concrete-FRP bonded interfaces. Two types of fiber fabrics: E-glass and Carbon are used, and a common epoxy resin is applied to bond the concrete-concrete and concrete-composite interfaces. Mode-I fracture tests of the 3PBB specimens for concrete-concrete, concrete-E-glass/epoxy composite, and concrete-Carbon/epoxy composite bonded interfaces are performed to determine the applied loads and load point displacements, from which critical strain energy release rates are obtained. The effect of loading rates on fracture toughness (in displacement control rates of 0.002 mm/sec, 0.01 mm/sec, and 0.05 mm/sec) is studied and discussed. Since there are very few test methods available to rigorously evaluate the interface bond fracture and integrity of concrete structures externally reinforced with FRP composites, the proposed experimental method can be efficiently used to evaluate interfaces for existing commercial combinations of concrete-FRP hybrid products and to obtain fracture toughness data useful for delamination studies under various environmental exposures and service loading.

Keywords: Mode-I fracture; concrete-FRP bonded interface; fracture toughness

Introduction

Current research on rehabilitation and strengthening of concrete structures has focused on the external bonding of FRP plates or fabrics to concrete, and significant increases in stiffness, strength and seismic response have been achieved by this technique that offers great potential for enhanced durability and service-life. However, there is a concern with the long-term reliable performance of the interface bond, which is critical in the application of this technology. The delamination of the interface can lead to premature failure of reinforced members, and therefore, there is a need to develop proven methods to characterize the performance of concrete-FRP interface bonds under static and cyclic loading combined with bond degradation effects due to environmental exposure.

In this section, the common test methods of Mode-I fracture using three-point bending beam (3PBB) specimens are briefly introduced, and previous studies on concrete-FRP bonded interface are reviewed.

Three-Point Bending Beam (3PBB) Specimens

Three-point bending beam (3PBB) specimens have been commonly applied to determine Mode-I fracture properties of concrete and rock materials. The fracture energy, G_c-values, for different concrete qualities were obtained by Petersson (1980) from three-point bending tests on notched beams, and the

stability conditions in the three-point bending test were determined by using a fictitious crack model. The results indicated that the critical fracture energy G_c was greatly influenced by the quality of the aggregate, the water-cement ratio and the age of the concrete. RILEM Committee on Fracture Mechanics of Concrete-Test Methods (1985) also recommended a 3PBB based method to obtain the fracture energy of mortar and concrete by means of three-point bending tests on notched beams. In this method, the data reduction procedures were mainly based on the fictitious crack model developed by Hillerborg et al. (1976 and 1989). Even though three fracture parameters: the fracture energy G_F, the material tensile strength f_t, and the critical crack separation displacement w_c, are needed in the fictitious crack model, only one parameter of fracture energy (G_F) is determined. The details of the RILEM recommendation are described and discussed by Hillerborg (1985 and 1989), and it is mainly based on a well defined physical model - fictitious crack model, which can be applied to all kinds of structures, regardless of whether a crack exists or not. The recommended test is size–dependent and easy to perform; therefore it is suitable to be implemented as a standard method. Later, RILEM Committee on Fracture Mechanics of Concrete-Test Methods (1990) developed a recommendation to determine fracture parameters (K_{Ic}^s and $\mathrm{CTOD_c}$) of plain concrete using three-point bending tests, which was based on the two-parameter fracture model by Jenq and Shah (1985). RILEM Committee on Fracture Mechanics of Concrete-Test Methods (1990) also proposed a recommendation to determine material fracture energy (G_f) using three-point bending tests, which was based on the size effect model by Bazant et al. (1987, 1990), in which different sizes of three-point bending beams were tested to obtain the fracture energy (G_f).

Fracture characterization of concrete and rock materials using the 3PBB specimens has been extensively conducted by several researchers. Palmer (1991) investigated fracture toughness, *R*-curve behavior, size effect and notch sensitivity of a low cement castable refractory with respect to temperature, and the results indicated that fracture toughness increases as temperature increases and span-to-depth ratio decreases. Yon (1991) used Moire interferometry to determine the crack opening displacements (COD) along propagating cracks in concrete 3PBB specimens. Shinohara (1991) developed an experimental method to obtain reliable load-displacement curves of plain concrete from the 3PBB tests, which included the post-peak softening behavior; a series of tests had been performed to investigate the influence of notch depth, loading rate, maximum aggregate size, water/cement ratio, crack propagation speed, and concrete aging upon the post-peak softening behavior. Zhang (1999) calculated the length of fracture process zone based on the load-deflection curve and acoustic emission characteristics of notched concrete 3PBB specimens with different notch depth. Xu (1999) proposed a new method to determine the double-*K* fracture parameters K_{Ic}^{ini} and K_{Ic}^{un} using the notched 3PBB specimens. Recently, Amparano (2000) investigated effect of aggregate content on fracture behavior of concrete using 48 geometrically similar 3PBB concrete specimens. A size effect method, in which the fracture behavior of concrete is characterized by two parameters: fracture energy G_f and effective fracture process zone c_f, was adopted to analyze the test data. The test results showed that with increasing volume fraction of aggregate, the compressive strength of concrete decreases slightly, fracture energy G_f varies within a small range, and the size of the fracture process zone becomes smaller.

Previous Studies on Concrete-FRP Fracture Toughness

Several researchers have used a fracture mechanics approach to characterize the fracture of concrete-composite bonded interfaces. Karbhari and Engineer (1996) used a peel test to determine the fracture toughness of interfaces between either carbon or glass composites bonded to concrete. By altering the peel angle as well as varying the loading speed, a number of tests were conducted to determine the fracture toughness of the interfaces. With an optimum loading speed of 5.08 mm/min and a peel angle of 45^o, the reported mode-I fracture toughness values for the glass and carbon composites are 382.52 J/m^2 and 477.87 J/m^2, respectively. Giurgiutiu et al. (1999) investigated the fracture

toughness of the interface bond between glass-composite overlays and concrete substrates. A cantilever beam specimen was used and the composite substrate was assumed to behave as a beam. After failing the specimens, the effectiveness of adhesion of the concrete-composite interface was determined by observing the amount of cement-paste residue remaining on the composite overlay. Surprisingly, their results indicated that the specimens with high fracture toughness values had a large portion of the cracks propagating within the concrete substrate, while those with lower fracture toughness values predominantly showed cracks propagating at the interface. A single contoured-cantilever beam specimen for carbon composite-concrete bonded interfaces was recently developed by Boyajian, Davalos and Qiao (2000), and values of G_{Ic} = 627 J/m^2 and G_{Ic} = 556 J/m^2 were reported using, respectively, the initial peak loads and the average peak load over the crack range (Boyajian et al. 2002).

In this study, the notched three-point bending beam (3PBB) specimens are adapted for fracture tests to characterize Mode-I fracture of concrete-FRP bonded interfaces. Both Carbon Fiber-Reinforced Polymer (GFRP) and Glass Fiber-Reinforced Polymer (CFRP) composites are used to produce the bonded interfaces. Three types of bonded interfaces (i.e., concrete-GFRP, concrete-CFRP, and concrete–concrete) are evaluated, and the corresponding fracture toughness values under Mode–I loading are obtained.

Experimental Procedures

Preparation of Specimens

To fabricate the 3PBB specimens for interface characterization, the end cross sections of two equal-size concrete beams were bonded with composite fabrics to form either concrete-CFRP or concrete-GFRP interfaces (Fig. 1). An initial central notch was created along the interfaces by using a cellophane insert. The concrete beams of dimension 100mm×100mm×450mm were made with the mix weight proportion 1.0:2.17:2.90 of cement, sand and aggregate. The maximum size of aggregates used is 18mm, and the water/cement ratio is 0.57. All the beams were removed from the molds 24 hours after casting and then were moisture cured at 72° F for 28 days before the 3PBB tests.

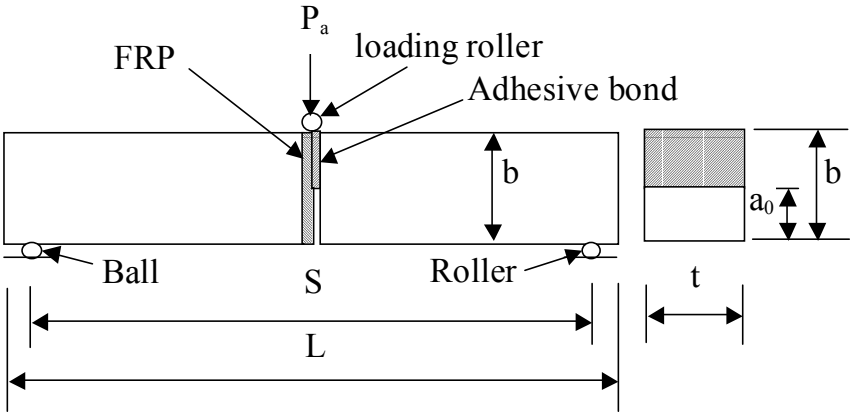

Figure 1. Three point bending beam (3PBB) specimen for Mode-I fracture test

Two kinds of fiber fabrics (i.e., E-glass and carbon) were used for the composite substrates which were bonded with concrete. The carbon fiber fabrics are Toray T700 12k tow sheet with thickness of 0.0065 in/ply (0.1651 mm/ply); while E-glass fibers used are cross-ply stitched fabrics (c-1800 fabrics from Brunswick Technologies, Inc., Maine). An off-the-shelf epoxy resin was used to first impregnate (wet) the fiber fabrics and then to bond the formed composite over the concrete. The epoxy-system 2000 used consists of two-part mixing components of resin and hardener.

A total of 18 concrete-CFRP 3PBB specimens were fabricated, and they were divided into three groups to evaluate the effect of loading rate on fracture toughness. Further, six concrete-GFRP 3PBB samples were manufactured, and for comparison purpose, additional six concrete-concrete bonded interface 3PBB specimens were also fabricated.

Test Procedures

The test configuration is shown in Fig. 1. A notch of half length of the beam height was created between the composite and concrete interface to define an initial crack length. A servo-hydraulic MTS was used to conduct the experiment, and the central applied load and load point displacement were recorded. A clip gage was used to accurately measure the load point displacement. For concrete-CFRP bonded interface, three loading rates of 0.002, 0.01, and 0.05mm/sec were employed in the displacement-controlled tests, and the effect of loading rates on fracture toughness measurement was assessed. While for concrete-GFRP and concrete-concrete bonded interface specimens, the loading rate of 0.01 mm/sec was applied.

Data Reduction

The fracture toughness or strain energy release rate G_F can be reduced from the measured load and load point displacement curve (P_a-δ_m curve) (Fig. 2). The self-weight of the beam cannot be neglected in the test, and the influence of beam self-weight can be accounted for by introducing an additional equivalent force P_w, which supplies the same amount of energy based on the load-displacement curve (see Fig. 2). Therefore the total load P applied on the beam can be represented as $P = P_w + P_a$, where P_a is the applied load, provided that the load and displacement are both applied downward. The total fracture energy W_t absorbed by the beam may be divided into three parts, W_0, W_1, and W_2, as shown in Fig. 2. In the physical test, only the P_a-δ_m curve can be recorded. The area under the measured $P_a - \delta_m$ curve is denoted as W_0; the rescaled P_a-δ curve will include the effect of beam self-weight, and the fracture energy due to the beam self-weight (W_1) is approximated as $W_1 = P_w\delta_0$ (where, δ_0 is the displacement corresponding to $P_a = 0$). As in the study conducted by Peterson (1981) and Swartz et al. (1988), W_2 is approximately equal to W_1. Therefore, the total fracture energy of the beam is expressed as

$$W_t = W_0 + 2P_w\delta_0 \tag{1}$$

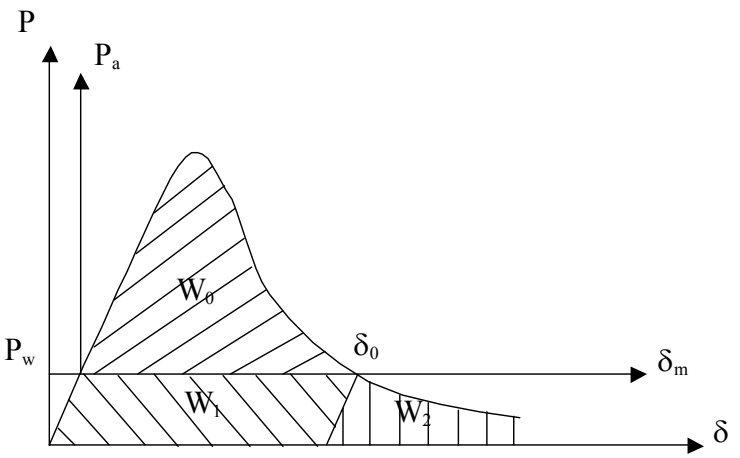

Figure 2. Load-displacement curve for evaluation of the fracture energy G_F

By assuming that energy absorption takes place only in the fracture zone, the fracture toughness or critical strain energy release rate (G_F) of the bonded interface can be calculated by

$$G_F = \frac{W_t}{(b-a_0)t} = \frac{W_0 + 2P_w\delta_0}{(b-a_0)t} \tag{2}$$

where, b is the depth of the beam, t is the width of the beam, and a_0 is the length of the notch). Based on this data reduction method, the critical strain energy release rate (G_F) of a notched 3PBB specimen can be obtained once the load-displacement of the specimen is recorded from the experiment.

Results and Discussion

Failure Behavior and Loading Response

The load vs. load point displacement curves for six concrete-CFRP interface specimens under respective three loading rates are plotted in Figs. 3 to 5. The average load-displacement relationships of six samples for different loading rate groups are shown in Fig. 6. As shown in Fig. 6, loading rate has little impact on load-displacement relationship, and the three load-rate groups have similar shapes and magnitudes of load vs. displacement curves. For concrete-GFRP and concrete-concrete bonded interface specimens, the constant intermediate rate of 0.01mm/sec was adopted in the 3PBB tests, and their corresponding load-displacement responses of six specimens are shown in Figs. 7 and 8. In comparison, the average load-displacement curves for three types of bonded interfaces under the load rate of 0.01mm/sec are shown in Fig. 9. As indicated in Fig. 9, the concrete-GFRP bonded interface assembly has the highest loading response, following by the concrete-concrete bonded interfaces. The concrete-CFRP bonded interfaces show the lowest loading resistance.

Interface Fracture Toughness

Based on the data reduction technique in Section 3, the fracture toughness or critical strain energy release rate (G_F) and critical load are obtained and given in Table 1. For concrete-CFRP interfaces, both the critical load and strain energy release rate increase with the increased rate. But the differences of fracture toughness among the three loading rates were not significant, which meant the fracture toughness was not evidently influenced by the loading rates at the given range. Also as shown in Table 1, the fracture toughness was proportional to the critical load. At a constant load rate of 0.01mm/sec, concrete-GFRP interface shows the highest fracture toughness, followed by concrete-concrete and concrete-CFRP bonded interfaces.

The surfaces of interface fracture along the bonding lines are also examined, and the percentages of adhesive failure (along the interface bond), cohesive failures in composite and concrete are provided in Table 2. It is observed that for concrete-CFRP bonded interface, the crack mostly propagated along the adhesive layer (interface failure) and never occurred in the composite, and some cohesive failure in concrete is observed; whereas the crack in concrete-GFRP bonded interface occurred mainly in the adhesive layers, but some cohesive failure in the composite was also observed. The fracture surface patterns for three types of the interfaces at the loading rate of 0.01mm/sec are shown in Figs. 10 to 12. As shown in Fig. 10, for concrete-CFRP bonded interfaces, the interface adhesive failure and concrete cohesive failure are dominant on the fractured surfaces. While for concrete-GFRP bonded interface (Fig. 11), all of three types of failure are present. For concrete-concrete interface (Fig. 12), almost equal interface adhesive and concrete cohesive failure are shown on the fractured surface.

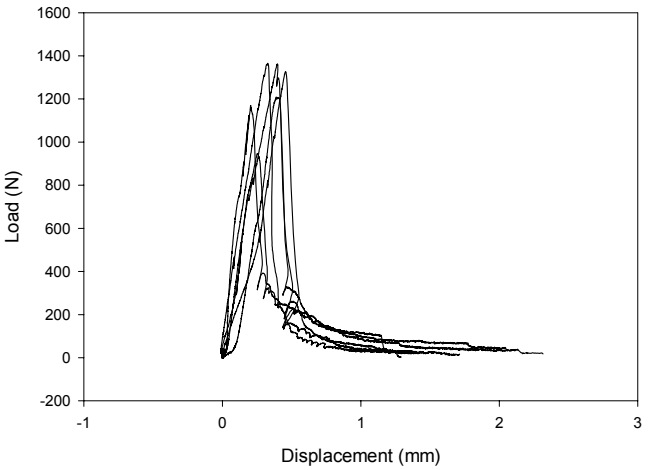

Figure 3. Load-displacement curves of concrete-CFRP interface specimens at loading rate = 0.002 mm/sec

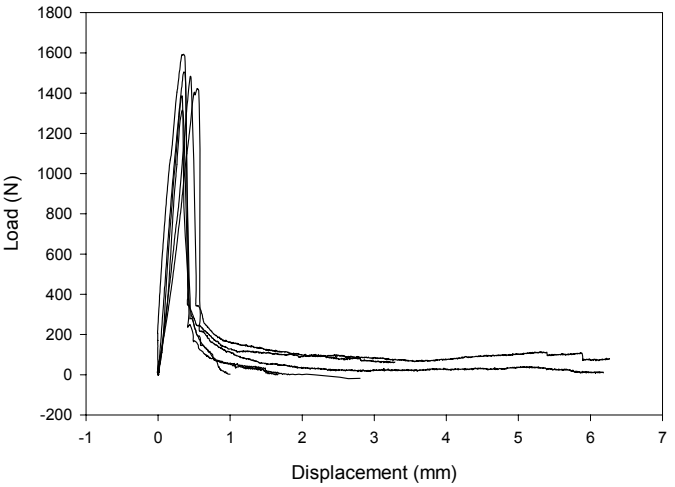

Figure 4. Load-displacement curves of concrete-CFRP interface specimens at loading rate = 0.01 mm/sec

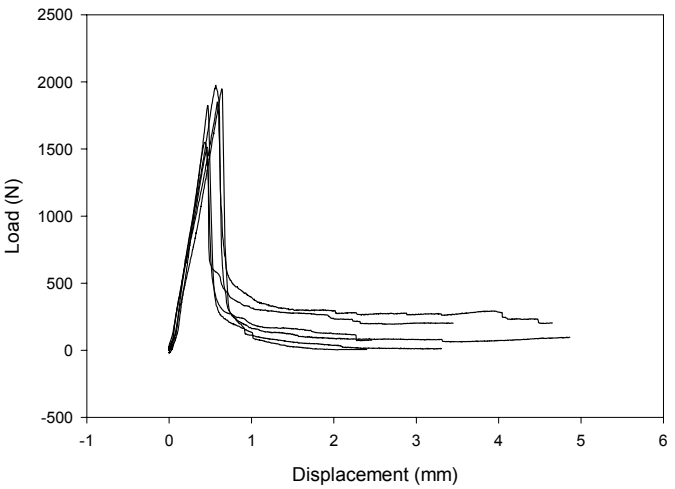

Figure 5. Load-displacement curves of concrete-CFRP interface specimens at loading rate = 0.05 mm/sec

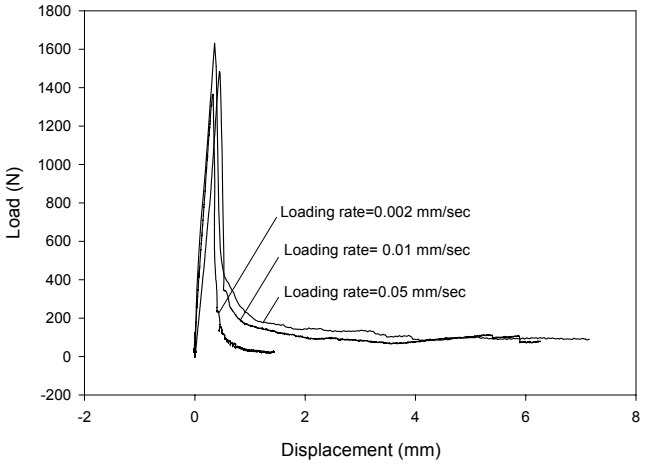

Figure 6. Comparison of load-displacement curves of concrete-CFRP interface specimens under different loading rates

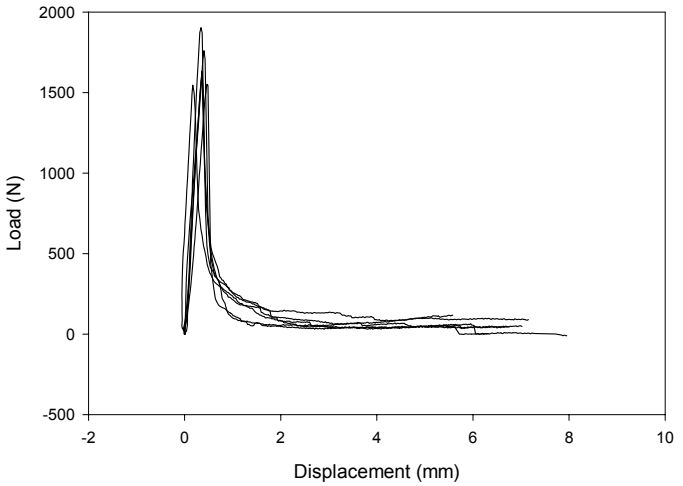

Figure 7. Load-displacement curves of concrete-GFRP interface specimen at loading rate = 0.01 mm/sec)

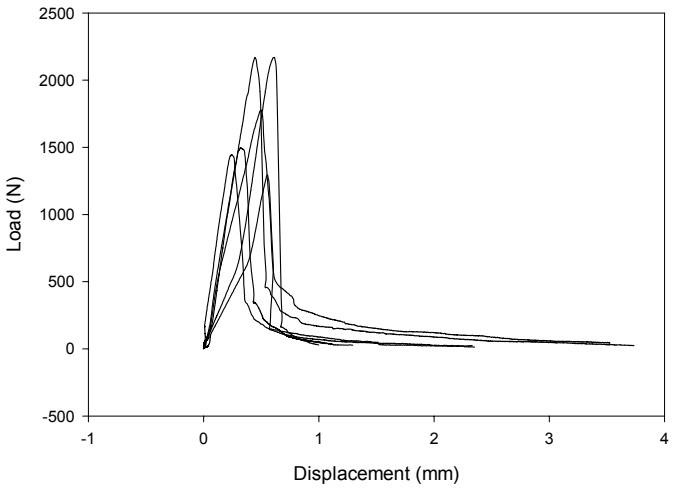

Figure 8. Load-displacement curves of concrete-concrete interface specimen at loading rate = 0.01 mm/sec

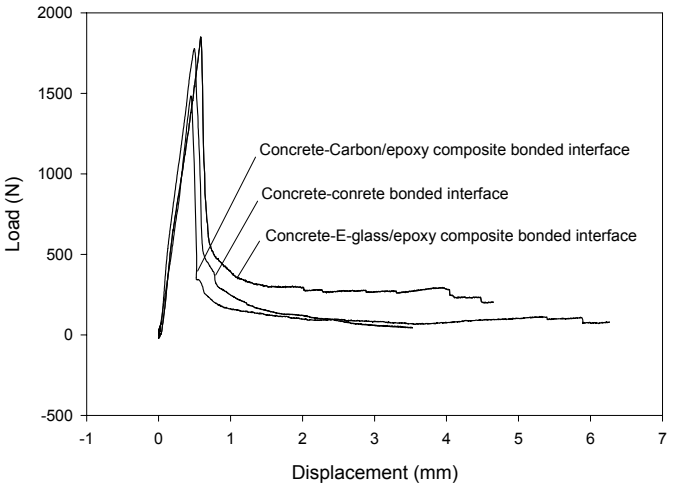

Figure 9. Comparison of load-displacement curves of three bonded interface specimens

Table 1. Strain Energy Release Rate G_F and the Critical Load P_{cr} of Bonded Interfaces

Bond types	Concrete-CFRP						Concrete-GFRP		Concrete-Concrete	
Loading Rate	0.002		0.01		0.05		0.01		0.01	
Specimen	P_{cr} (N)	G_F (N/m)	P_{cr} (N)	G_F (N/m)	P_{cr} (N)	G_F (N/m)	P_{cr} (N)	$\mathbf{G_F}$ (N/m)	P_{cr} (N)	G_F (N/m)
1	1361	112	1503	116	1761	161	1948	200	1294	132
2	1210	118	1592	139	1552	150	1975	201	1779	188
3	1326	135	1317	101	1615	160	1824	143	2171	199
4	947	78	1388	113	1904	163	1850	200	2135	190
5	1170	97	1423	147	1548	138	1548	145	1446	100
6	1361	138	1486	133	1632	154	1512	175	1490	118
Avg	1229	113	1452	125	1669	154	1776	177	1719	155
Cov	0.130	0.202	0.067	0.141	0.083	0.061	0.112	0.156	0.216	0.277

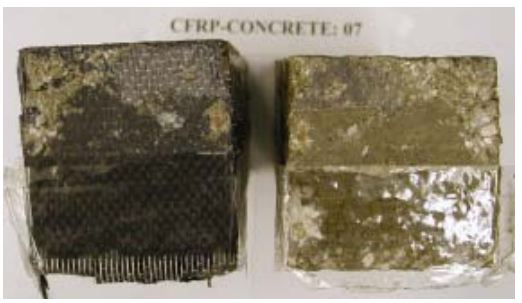

Figure 10. Fractured surfaces of concrete-CFRP bonded interface

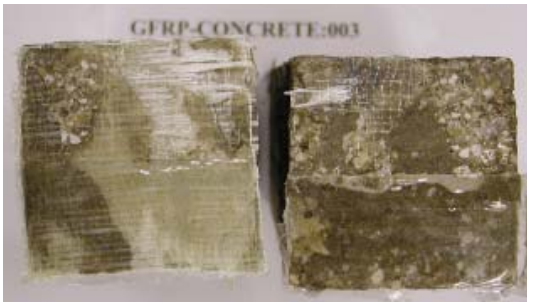

Figure 11. Fractured surfaces of concrete-GFRP bonded interface

Figure 12. Fractured surfaces of concrete-concrete bonded interface

Table 2. Failure Percentage (%) of Bonded Interfaces

Bond types	Concrete-CFRP									Concrete-GFRP			Concrete-Concrete	
Rate	0.002 mm/sec			0.01 mm/sec			0.05 mm/sec			0.01 mm/sec			0.01 mm/sec	
Failure	F_{ad}	F_{con}	F_{com}	F_{ad}	F_{con}	F_{com}	F_{ad}	F_{con}	F_{com}	F_{ad}	F_{con}	F_{com}	F_{ad}	F_{con}
1	90	10	0.0	23	77	0.0	95	5	0.0	35	40	25	90	10
2	65	35	0.0	10	90	0.0	80	15	5	15	75	0.0	14	86
3	85	15	0.0	93	07	0.0	98	2	0.0	20	45	35	80	20
4	93	7	0.0	97	3	0.0	70	30	0.0	60	25	15	20	80
5	74	26	0.0	25	75	0.0	77	23	0.0	70	25	5	0.0	100
6	76	24	0.0	72	28	0.0	75	25	0.0	30	70	0.0	33	67

Note: F_{ad} - Adhesive failure; F_{con} - Concrete failure; F_{com} - Composite failure.

Conclusions

In the present study, a conventional test method using a three-point bending beam (3PBB) specimen was adapted to characterize Mode-I fracture of concrete-FRP bonded interfaces. Two types of fiber fabrics: E-glass and Carbon were used, and a commercial epoxy resin was applied to bond the concrete-concrete and concrete-composite interfaces. Mode-I fracture tests are performed using the 3PBB specimens for concrete-CFRP, concrete-GFRP, and concrete-concrete bonded interfaces, and the applied loads and load point displacements are recorded, from which the critical strain energy release

rates were computed. The effect of loading rates (in displacement control rates of 0.002 mm/sec, 0.01 mm/sec, and 0.05 mm/sec) on fracture toughness measurement of concrete-CFRP bonded interface was studied. The critical loads and critical strain energy release rates (G_F) of concrete-CFRP interface increase as the loading rate increase, but the differences of fracture toughness under the given loading rate ranges were not significant, which meant that the fracture toughness was not evidently influenced by the loading rates. The test results also indicated that the fracture toughness was proportional to the critical load. Compared to the concrete-CFRP bonded interface, the critical load and critical fracture toughness (G_F) of concrete-GFRP bonded interface were relatively higher. The adapted experimental method using the 3PBB specimen can be efficiently used to evaluate interfaces for combinations of concrete-FRP hybrid products and to obtain fracture toughness data. We must note that the fracture toughness values reported are not for commercial composite-concrete products, as given in Karbhari and Engineer (1996) and Boyajian et al. (2002). Further studies of size effect and commercial bonding systems using the 3PBB specimens are in progress.

Acknowledgements

This study was partially supported by the University of Akron and the National Science Foundation (CMS-0002829 under program director Dr. Ken P. Chong).

References

1. Amparano, Felix E., Xi, Y. and Roh, Y. S. "Experimental study on the effect of aggregate content on fracture behavior of concrete", Engineering Fracture Mechanics , Vol. 67 , 2000, pp. 65-84.
2. Bazant, Z. P., and Pfeiffer, P. A., "Determination of Fracture Energy from Size Effect and Brittleness Number," ACI Materials Journal, Vol.84, No. 6, 1987, pp. 463-480.
3. Bazant, Z. P., and Kazemi, M. T., "Determination of Fracture Energy, Process Zone Length and Brittleness Number from Size Effect, with Application to Rock and Concrete," International Journal of Fracture, Vol. 44, 1990, pp. 111-131.
4. Boyajian, D., Davalos, J.F., and Qiao, P.Z., "Development of a Test Specimen for FRP-Concrete Mode-I Fracture," In Proceedings of the *3nd Int. Conf. on Advanced Composite Materials in Bridges and Structures (ACMBS III)*, Ottawa, Ontario, Canada, 2000, pp. 445-452.
5. Boyajian, D., Davalos, J.F., Ray, I., and Qiao, P.Z., "Evaluation of interface fracture of concrete externally reinforced with FRP," In 2*nd Int. Conf. on Durability of FRP Composites for Construction (CDCC2002)*, Montreal, Quebec, Canada, May 29-31, 2002, submitted.
6. Jeng, Y. S., and Shah, S. P., "A Two Parameter Fracture Model for Concrete," Journal of Engineering Mechanics, Vol. 111, No. 4, 1985, pp. 1227-1241.
7. Giurgiutiu, V., Lyons, J., Petrou, M., Laub, D. and Whitley, S. "Experimental Fracture Mechanics for the Bond between Composite Overlays and Concrete Substrate," Proceedings of the International Composites Expo (ICE), Cincinnati, OH, 1999, pp. 4D(1-6).
8. Hillergorg, A., Modeer, M., and Petersson, P.-E., "Analysis of Crack Formation and Crack Growth by Means of Fracture Mechanics and Finite Elements, " Cement and Concrete Research, Vol. 6, 1976, pp. 773-782.
9. Hillergorg, A., "Results of Three Comparative Test Series for Determining the Fracture Energy G_F of Concrete," Materials and Structures, Vol. 18, No. 107, 1985, p. 407-413.
10. Hillergorg, A., "Existing Methods to Determine and Evaluate Fracture Toughness of Aggregative Materials: RILEM Recommendation on Concrete," in Fracture Toughness and

Fracture Energy, Test Methods for Concrete and Rock, edited by Mihashi, H. ,et al., Balkema, Rotterdam, 1989, pp. 145-151.
11. Karbhari, V.M. and Engineer, M. "Investigation of Bond between Concrete and Composites: Use of a Peel Test," J. of Reinforced Plastics and Composites, 15, 1996, pp. 208-227.
12. RILEM Committee on Fracture Mechanics of Concrete-Test Methods, "Determination of the Fracture Parameters(K_{Ic}^{s} and $CTOD_c$) of plain concrete using three-point bending tests", Materials and Structures , Vol. 23,1990, pp. 457-460.
13. RILEM Committee on Fracture Mechanics of Concrete-Test Methods, "Determination of the Fracture Energy of Mortar and Concrete by Means of Three-Point Bend Tests on Notched Beams", Materials and Structures , Vol. 18, No. 106,1985, pp. 285-290.
14. RILEM Committee on Fracture Mechanics of Concrete-Test Methods, "Size Effect Method for Determining the Fracture Energy and Process Zone Size of concrete", Materials and Structures , Vol. 23,1990, pp. 461-465.
15. Palmer, G. B., and Baker, G., "Fracture toughness and size effect in low-cement refractories", in Fracture Processes in Concrete, Rock, and Ceramics, edited by Mier, J.G. M. van, et al, Noordwijk, The Netherlands, Vol. 1, pp. 387-396.
16. Petersson, P. E., "Fracture Energy of Concrete: Practical Performance and Experimental Results", Cement and Concrete Research, Vol. 10, pp. 91-101.
17. Petersson, P. E., "Crack growth and development of fracture zones in plain concrete and similar materials", Report TVBM-1006, Division of Building Materials, Lund Institute of Technology, 1981.
18. Shinahara, Y., Furumura F. and Abe, T, "Softening Behavior of Concrete in Three-Point Bend Tests of Single Edge Notched Beams", in Fracture Processes in Concrete, Rock, and Ceramics, edited by Mier, J.G. M. van, et al, Noordwijk, The Netherlands, Vol. 2, pp.523-532.
19. Swartz, S. E., and Yap, S. T., "The influence of dead load on fracture energy measurements using the RILEM Method", Materials and Structure, Vol. 21, 1988, pp410-415.
20. Xu, S., and Reinhardt, H. W., "Determination of Double-K Criterion for Crack Propagation in Quasi-brittle Fracture, Part 2: Analytical Evaluating and Practical Measuring Methods for Three-Point Bending Notched Beams", International Journal of Fracture, Vol. 98, 1999, pp. 151-177.
21. Yon, J. H., Hawkins, N. M., Guo, Z. K. and Kobayashi, A. S., "Fracture Process Zone Associated With Concrete Fracture", in Fracture Processes in Concrete, Rock, and Ceramics, edited by Mier, J.G. M. van, et al, Noordwijk, The Netherlands, Vol. 2, pp.485-494.
22. Zhang, D. and Wu, K. "Fracture Process Zone of Notched Three-Point-Bending Concrete Beams", Cement and Concrete Research, Vol. 29, 1999, pp. 1887-1892.